IEEE Access
Multidisciplinary | Rapid Review | Open Access Journal

Received 20 November 2024, accepted 8 January 2025, date of publication 14 January 2025, date of current version 22 January 2025.

Digital Object Identifier 10.1109/ACCESS.2025.3529768

RESEARCH ARTICLE

Vehicle-to-Vehicle Communication Channel Estimator Based on Gate Recurrent Unit

JUN-HAN WANG[1], HE HE[1], KOSUKE TAMURA[1], (Graduate Student Member, IEEE), SHUN KOJIMA[2], (Member, IEEE), JAESANG CHA[1], AND CHANG-JUN AHN[1], (Senior Member, IEEE)

[1]Graduate School of Engineering, Chiba University, Chiba 263-8522, Japan
[2]Institute of Industrial Science, The University of Tokyo, Tokyo 113-8654, Japan

Corresponding author: Jun-Han Wang (cdda5211@chiba-u.jp)

This work was supported in part by the Japan Science and Technology Agency Broadening Opportunities for Outstanding Young Researchers and Doctoral Students in Strategic Areas (JST BOOST), Japan, under Grant JPMJBS2413; and in part by the Grant of Scientific Research from the Japan Society for the Promotion of Science (JSPS), Telecommunications Advancement Foundation (TAF) Foundation, Suzuki Foundation, Chubu Science and Technology Center, and Takahashi Industrial and Economic Research Foundation under Grant 22K04085.

ABSTRACT With the development of autonomous vehicle operation, vehicle-to-vehicle (V2V) communication plays an increasingly important role. However, in high-speed mobile environments, the channel has fast time-varying, which significantly decreases the property of channel estimation. On the other hand, the frame structure of the IEEE 802.11p standard contains a few number of pilots and a large pilot interval, which is not sufficient to track the rapidly changing channel environment accurately. In recent years, deep learning has been widely used for channel estimation. However, these methods typically perform poorly in high-speed mobility scenarios or have excessively high computational complexity. To alleviate such issues, this study proposes a channel estimation method by combining the sparrow search algorithm (SSA) and gated recurrent unit (GRU). In addition, this paper adds the attention mechanism to GRU to improve the robustness of the model. The computer simulation results confirm that, compared to traditional schemes, the proposed estimator can achieve a lower bit error rate (BER) and normalized mean squared error (NMSE). At the same time, the computational complexity of the algorithm has been reduced to some extent, allowing the estimator to complete the channel estimation faster. This study provides a useful reference for optimizing neural networks and thus improving the performance of channel estimators.

INDEX TERMS Vehicle-to-vehicle, channel estimation, SSA, GRU, attention, IEEE 802.11p.

I. INTRODUCTION

Vehicle communication technology plays a crucial role in modern intelligent transportation systems [1], [2], [3], [4]. Accurate and efficient vehicle communication technology promotes information exchange between vehicles and improves transportation safety, efficiency, and convenience [5]. However, the dual selective nature of vehicular channels, especially the rapid changes in high mobility scenarios, makes channel estimation a challenging task.

To enhance vehicular communications, researchers have extensively explored channel assignment and coordination techniques. Prior work has explored improving vehicular communications through channel assignment and coordination. For instance, the adaptive multi-channel assignment and coordination (AMAC) scheme [6] introduces an adaptive multi-channel allocation approach, which leverages channel state information (CSI) to reduce congestion and improve overall network performance. Johari et al. [7] proposed a channel assignment method based on the Markov model, improving resource utilization and reducing transmission collision. While channel assignment strategies are critical for resource management and interference mitigation, they have inherent limitations in addressing the dynamic nature of the vehicular communication environment. Even with optimal channel selection, vehicular communication channels' rapidly changing channel conditions, including fading, noise, and interference, remain challenges that channel assignment cannot overcome alone.

The associate editor coordinating the review of this manuscript and approving it for publication was Olutayo O. Oyerinde.

In vehicular communication, channel estimation is a crucial aspect, and its accuracy directly affects the communication quality and the success of data transmission. Channel estimation schemes in vehicular communication scenarios, especially for the IEEE 802.11p standard, fall into two main categories. The first category is the scheme that modifies the IEEE 802.11p [8] standard for channel estimation. For example, Nagalapur et al. [9] adds complementary training symbols to IEEE 802.11p frames to improve the pilot density and solve the unreasonable pilot distribution problem. Kim et al. [10] proposed a mid-amble aided channel estimation method, which improves the accuracy of the estimation but has the disadvantage that excessive training sequences reduce the spectral efficiency. The second category is a channel estimation scheme that retains the IEEE 802.11p standard. In order to solve the problem of a low number of pilots in the IEEE802.11p standard, authors of [11], [12], and [13] utilize the data pilot aided (DPA) method for channel estimation. The core idea is to estimate the current channel by using the previously estimated data signals as data pilots. However, since this is an iterative process, the error in the previous estimation is gradually amplified, thus affecting the accuracy of the subsequent estimation. Fernandez et al. [14] utilizes the idea of decision feedback to propose a spectra temporal averaging (STA) scheme, which performs smoothing in the time and frequency domains to improve the channel estimation performance. However, the scheme is based on the iterative update of decision feedback, and the update parameters are difficult to obtain accurately. To solve the above problem, Zhao et al. [15] proposes a constructed data pilot (CDP) scheme using the channel correlation property between adjacent data symbols, which determines whether to update the channel or not by judging the reliability of the channel frequency response (CFR). Based on the CDP method, Kim et al. [16] proposes a time-domain reliability test frequency-domain interpolation (TRFI) scheme that performs well in high-order modulation schemes and high-mobility environments. The former of the above two methods lack robustness in high-mobility moving environments, while the latter relies on assumptions for many of its processes and has poor practical applicability. Previous research has shown that, in the face of complex vehicular communication channels, traditional algorithms usually find it difficult to adapt to the rapidly changing channel environment.

In recent years, machine learning has been utilized successfully in a number of fields. Among them, capabilities such as strong generalization and ease of application of deep learning methods make them suitable for integration into communication systems. For example, to solve the nonlinear distortion problem in communication systems, [17] proposes a method to implicitly estimate the CSI and directly recover the transmitted symbols via deep neural networks (DNN). On the other hand, [18] first performs initial feature extraction using a conventional linear model, and then further performs channel estimation via a shallow neural network to keep the nonlinear distortion. This proves that neural networks are more robust in non-ideal states, but simple neural networks are difficult to meet the communication environment of complex vehicular communication networks. HE et al. [19] proposed a channel estimation method based on a convolutional neural network (CNN) and showed that the deep learning method could significantly improve the performance compared with the traditional algorithm. However, since channel information is essentially sequential, natural language processing (NLP) methods that are more adept at dealing with sequential problems would be better suited to the channel detection problem [20], [21], [22]. Gizzini et al. [23] proposed a channel detector based on a long short-term memory unit (LSTM), proving the advantage of LSTM over DNN in high mobility environments. However, LSTM usually needs to improve with large-scale training datasets and offers limited improvement in accuracy in high-speed scenarios. Pan et al. [24] proposed a network combining a multilayer perceptron network (MLP) and LSTM, achieving superior results. However, at the same time, the computational complexity was greatly increased. Similarly, Zhou et al. [25] proposed a channel prediction model combining CNN and LSTM for the high-speed railway communication environment with more complex channel conditions. Experimental results show that the composite model can indeed achieve higher prediction accuracy compared to a single model. Still, the computational complexity also increases exponentially, which is unacceptable for vehicle communication channels with real-time requirements. In contrast, Yin et al. [26] and Unnisa et al. [27] use heuristic algorithms to optimize the network model, which improves the efficiency of the model without increasing its complexity. However, these methods have been validated mainly in low-speed or static environments. They may lack sufficient ability to cope with the fast time-varying characteristics of the channel in high-mobility environments. The convergence speed and computational resource requirements still need to be further optimized for real-time V2V communication in practice.

In order to make the LSTM-MLP estimator more concise and improve the performances such as BER and NMSE, this paper proposes an estimator based on the gated recurrent unit optimized by attention mechanism for channel estimation. In addition, a sparrow search algorithm is used to optimize the GRU network to further improve the accuracy and generality of the model. By utilizing GRU to correct the errors in the DPA process, the proposed method effectively improves the performance of channel estimation in high-mobility environments while reducing the computational complexity. The contributions of this paper are summarized as follows:

1) We introduce a novel channel estimation approach that combines metaheuristic algorithms with neural network techniques to enhance estimation accuracy in high-mobility vehicular environments. Unlike conventional deep learning-based estimators, which often suffer from high computational complexity, our approach

TABLE 1. List of symbols and definitions.

Symbol	Definition
$y(n)$	received signal
$h(n,l)$	time-varying multipath impulse response
$w(n)$	Gaussian white noise
σ^2	noise variance
$X(k)$	frequency-domain transmit signal
$H(k)$	channel frequency response
$W(k)$	frequency-domain form of the noise
L	paths' number
N	subcarriers' number
$X_T(k)$	training symbol in predefined preamble
$Y_T(k)$	received signals in frequency-domain
$D_i(k)$	received signal of the i-th OFDM symbol
$\hat{X}_i(k)$	the i-th OFDM symbol
$\tilde{H}_i(k)$	initial channel response estimate of the i-th symbol
K_d	data subcarrier
K_p	pilot subcarrier
$Q(\cdot)$	demap operation
$Y_i(k)$	the i-th received OFDM symbol
x_t	input
z_t	update gate
r_t	reset gate
σ	sigmoid function
W	weight matrix
b	bias
h_t	hidden state
$\tilde{h_t}$	candidate hidden state
$\odot$	Hadamard product
x_i	input of the i-th GRU unit
h_{GRU_i}	the CSI predicted by GRU
h_i	the CSI predicted by LS
Θ	parameters in the GRU
E_t	attention probability distribution value
S_i	attention weight value
r_i	output value of the attention mechanism
$\hat{H}$	final result of the channel estimation
x	individual sparrows
d	number of hyperparameters
n	sparrows' number
$f(\cdot)$	fitness function
Q	standard normally distributed random number
R	uniform random number in $[0, 1]$
VT	vigilance threshold
β	standard normally distributed random number
xw	current worst sparrow position
xb	current best sparrow position
f_i	present individual
f_g	global optimal fitness
D	number of columns of the matrix

leverages the strengths of metaheuristic optimization to refine neural network performance. This integration allows the model to adapt efficiently to the rapidly changing nature of vehicular channels while reducing computational demands, making it particularly suited for real-time V2V applications.

2) We develop a two-stage channel estimation scheme, where the offline training phase optimizes model parameters using extensive data, while the online estimation phase achieves real-time performance through pre-trained models. By separating training and estimation, our method minimizes the processing load during real-time operations, making it efficient for practical V2V systems. Simulation results show that our proposed method outperforms conventional and state-of-the-art estimators in high-mobility scenarios, offering a reliable and low-complexity solution for modern V2V communication systems.

TABLE 2. List of abbreviations used in the paper.

Abbreviation	Definition
V2V	vehicle-to-vehicle
SSA	sparrow search algorithm
GRU	gated recurrent unit
BER	bit error rate
AMAC	adaptive multi-channel assignment and coordination
DPA	data pilot aided
STA	spectra temporal averaging
CDP	constructed data pilot
TRFI	test frequency-domain interpolation
DNN	deep neural network
CNN	convolutional neural network
NLP	natural language processing
LSTM	long short-term memory unit
MLP	multilayer perceptron network
ICI	inter-carrier interference
LS	least squares
CSI	channel state information
CFR	channel frequency response
TDL	tapped delay line
VTV-SDWW	vehicle-to-vehicle same direction with wall
VTV-UC	vehicle-to-vehicle urben canyon
ISI	inter-signal interference
MAC	multiply-accumulate

The rest of this paper is organized as follows: Section II describes the IEEE802.11p standard, the DPA process, and the structure of the GRU. The details of the proposed SSA-GRU-Att estimator are elaborated in Section III. Section IV gives the performance comparison results of the proposed method with other estimators, and finally, Section V concludes this paper. Symbols, definitions, and abbreviation are given in Table 1 and Table 2.

II. SYSTEM MODEL

A. IEEE 802.11P STRUCTURE

IEEE 802.11p, derived from IEEE 802.11a, changes the frequency band in which the system is located in the range of 5.0 GHz to 5.9 GHz and the bandwidth from 20 MHz to 10 MHz to overcome inter-symbol interference caused by increased multipath delay in the automotive communications environment. As shown in Fig. 1, each packet consists of a preamble, a signal field, and a data field. The signal field conveys the packet information, and the data field carries the payload containing the data symbols. Its physical layer is based on OFDM technology with 64 subcarriers per OFDM symbol. which includes 4 pilot subcarriers, 12 null subcarriers, and 48 data subcarriers.

The received signal $y(n)$ of the OFDM-based IEEE 802.11p system in the time domain through the fading channel is described as

$$y(n) = \sum_{l=0}^{L-1} h(n,l)x(n-l) + w(n), \tag{1}$$

where $h(n, l)$ is the time-varying multipath impulse response, L refers to the paths' number, and $w(n)$ stands for the

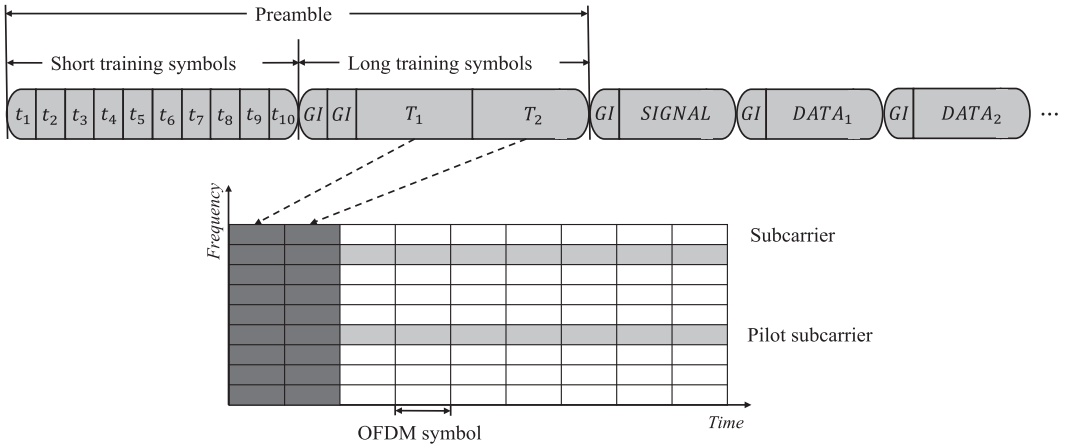

FIGURE 1. IEEE 802.11p packet structure. (Adapted from [24]).

Gaussian white noise with a noise variance of σ^2. In [16], it has shown that the Doppler shift of the V2V channel is not sufficient to cause serious inter-carrier interference (ICI) problems. Therefore, in this work, the effect of ICI is ignored. After removing the cyclic prefix at the receiver side and applying the discrete Fourier transform, the signal that is received in the frequency domain is expressed as

$$\begin{aligned} Y(k) &= \frac{1}{\sqrt{N}} \sum_{n=0}^{N-1} y_n e^{j2\pi nk/N} \\ &= X(k)H(m) + W(m), \quad (m = 0, 1, \ldots, N-1) \end{aligned} \tag{2}$$

where X_m is the frequency-domain transmit signal, H_m is the channel frequency response, W_m represent the frequency-domain form of the noise, and N is the subcarriers' number. For the k-th subcarrier, the m-th symbol in a frame, Eq. (2) can be written as

$$Y_m(k) = X_m(k)H_m(k) + W_m(k). \tag{3}$$

B. CHANNEL ESTIMATION METHOD BASED ON DPA

The signal propagation environment is intricate and complex in vehicular wireless communication scenarios, so the channel has an obvious multipath effect. At the same time, both the transmitter and receiver are in high-speed motion, which also induces a Doppler shift in the signal. In the frame structure of the IEEE 802.11p standard, the number of pilots is limited and fixed. If more pilots are inserted, the structure of the IEEE 802.11p standard will be damaged, and the spectral efficiency will be affected, which leads to the fact that the traditional channel estimation schemes can hardly achieve satisfactory results in vehicular communication scenarios. In order to solve the above problems, the channel estimation scheme of DPA has been widely researched, and its core idea is to estimate the channel frequency response at the current moment by treating the OFDM data symbols after demapping at the previous moment as the pilot.

The first step is to compute the initial channel estimate using the least squares (LS) algorithm based on the two long training symbols in the preamble:

$$\tilde{H}_0(k) = \frac{Y_{T_1}(k) + Y_{T_2}(k)}{2X_T(k)}, \tag{4}$$

where $X_T(k)$ is the training symbol in predefined preamble, $Y_{T_1}(k)$ and $Y_{T_2}(k)$ represent the received signals in frequency-domain. For the first OFDM symbol received, equalization is performed according to the initial channel estimate $\tilde{H}_0(k)$:

$$D_1(k) = \frac{Y_1(k)}{\tilde{H}_0(k)}. \tag{5}$$

Then, the equalized symbols are demapped to obtain the transmit symbol correction value:

$$\hat{X}_1(k) = \begin{cases} Q[D_1(k)] & \text{if } k \in K_d \\ X_T(k) & \text{if } k \in K_p, \end{cases} \tag{6}$$

where K_d and K_p represent the data subcarrier and the pilot subcarrier, respectively. $Q(\cdot)$ denotes the operation of demap to the nearest constellation point. The channel response estimate for the first OFDM symbol is then re-estimated using the LS algorithm by considering $\hat{X}_1(k)$ as the pilot at the current moment:

$$\tilde{H}_1(k) = \frac{Y_1(k)}{\hat{X}_1(k)}. \tag{7}$$

By analogy, for the i-th received OFDM symbol $Y_i(k)$, the channel response estimate $\tilde{H}_{i-1}(k)$ of the $i-1$-th OFDM symbol is used for equalization, and the channel estimate is calculated. As the DPA process iterates, the error generated by the estimation of the previous symbols is gradually amplified, which affects the estimation of the subsequent symbols, thus constraining the accuracy of the channel estimation.

C. GATED RECURRENT UNIT NETWORK

Since the error propagation problem severely constrains the accuracy of DPA channel estimation, GRUs are used to correct errors in the DPA process. Each GRU unit includes

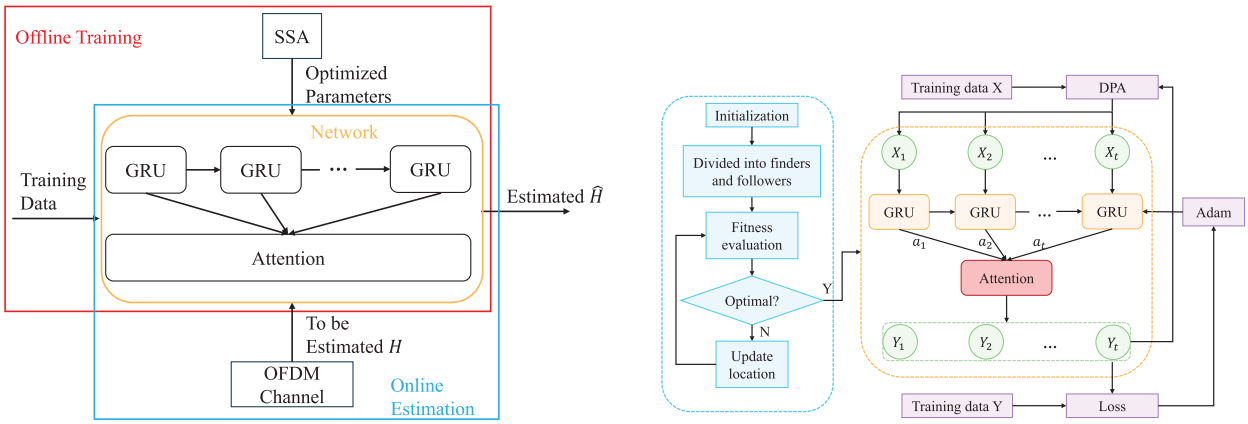

(a) The division between offline training and online estimation.

(b) Structure of the proposed SSA-GRU-Att channel estimator.

FIGURE 2. Training process and structure of the proposed channel estimator.

an update gate z_t and a reset gate r_t, and the parameters of each GRU unit are shared; That is, the neural network parameters are the same at every time step. The GRU network can hold the previous inputs in order to predict the channel state information at the next moment. The principle of the GRU unit is expressed as [28]:

$$\begin{aligned} z_t &= \sigma(W_z \cdot [h_{t-1}, x_t] + b_z) \\ &= \sigma(W_{zh} h_{t-1} + W_{zx} x_t + b_z), \end{aligned} \tag{8}$$

$$\begin{aligned} r_t &= \sigma(W_r \cdot [h_{t-1}, x_t] + b_r) \\ &= \sigma(W_{rh} h_{t-1} + W_{rx} x_t + b_r), \end{aligned} \tag{9}$$

$$\begin{aligned} \tilde{h_t} &= \tanh(W_h \cdot [r_t \odot h_{t-1}, x_t] + b_h) \\ &= \tanh(W_{hh}(r_t \odot h_{t-1} + W_{hx} x_t) + b_h), \end{aligned} \tag{10}$$

$$h_t = h_{t-1} \odot z_t + \tilde{h_t} \odot (1 - z_t), \tag{11}$$

where σ stands for sigmoid, W and b mean the weight matrix and bias learned through training. r_t and z_t refer to reset gate and update gate, h_t and $\tilde{h_t}$ means the hidden state and candidate hidden state at moment t, respectively. $\odot$ represents Hadamard product, and tanh is the activation function.

The reset gate controls how much of h_{t-1} flows into $\tilde{h_t}$. Specifically, if the value of r_t approaches 0, it implies that most of the hidden state from the former step is discarded. The opposite means that most of the hidden state is retained. Thus, the reset gate can ignore historical information irrelevant to the current prediction information.

The update gate controls how much h_{t-1} and x_t flow into h_t. The larger the value of z_t, the more h_{t-1} flows into h_t. Conversely, more x_t flows into h_t. If the value of the update gate has been close to 1 since many time steps ago, then it can be approximated that this historical information has been preserved and passed on to the current time step. This facilitates capturing long-term dependencies in the time series.

III. PROPOSED SSA-GRU-ATTENTION ESTIMATOR

As mentioned earlier, traditional channel estimation algorithms are no longer applicable in high-speed environments. In order to solve this problem, this paper proposes a high-speed channel estimation method that utilizes the powerful capabilities of GRU to process sequence data that tracks changes in the channel.

A. NETWORK ARCHITECTURE

The proposed method is divided into two stages. Firstly, as shown in Fig 2(a), this work trains the proposed network using a sufficient amount of channel data collected, and the network parameters are tuned using SSA so that the network learns the channel features adequately. This process is called offline training. Then, this work feedbacks the OFDM subframe-sized channel matrix into the trained network and continuously predicts the CSI, which is called online estimation. Putting the training process offline makes full use of large datasets and high-performance computing resources and greatly reduces the burden of computation and delay during online estimation, ensuring real-time and reliable estimation. The proposed network consists of multiple GRU units connected in series, and its structure is shown in Fig 2(b).

The data flow of the proposed GRU estimator can be seen in Fig 3. The input data and channel estimation are described in detail below. The input of the proposed network is a subframe-sized CSI matrix $H \in \mathbb{R}^{T \times L}$, and the GRU processes the data of only one symbol at each time step. The GRU network requires time-series data as inputs, so we utilize Eq.4 to get the initial channel frequency response.

According to the DPA process, the received signal of the i-th OFDM symbol is equalized through the initial channel of the $i-1$-th OFDM symbol accordingly:

$$D_i(k) = \frac{Y_i(k)}{\tilde{H}_{i-1}(k)}, \tag{12}$$

then the i-th OFDM symbol can be written as:

$$\hat{X}_i(k) = \begin{cases} Q[D_i(k)] & \text{if } k \in K_d \\ X_T(k) & \text{if } k \in K_p. \end{cases} \tag{13}$$

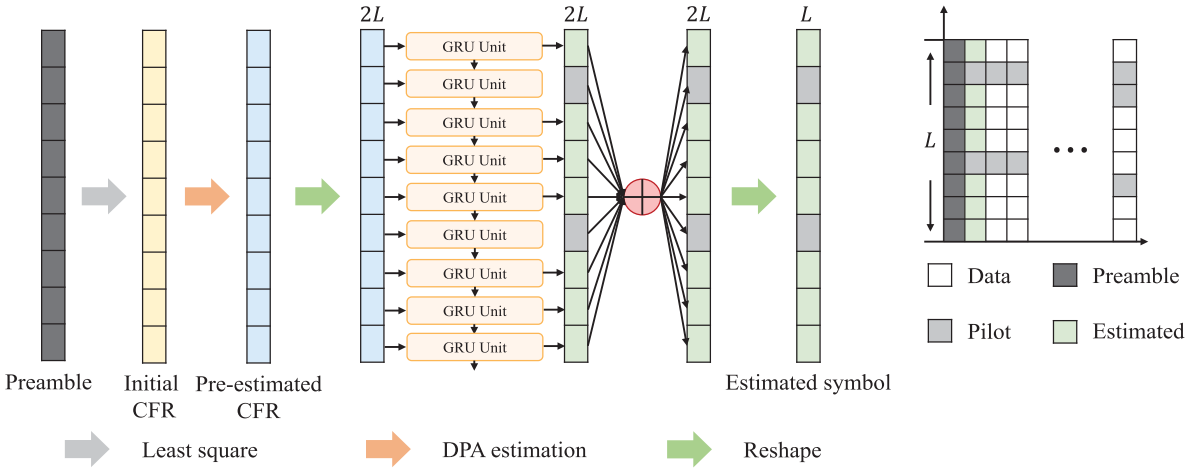

FIGURE 3. Data flow of the proposed GRU network.

Then, the initial channel response estimate for the k-th subcarrier of the i-th symbol can be expressed as:

$$\tilde{H}_i(k) = \frac{Y_i(k)}{\hat{X}_i(k)}. \tag{14}$$

Since the channel data are complex signals, the data must be preprocessed before being fed into the proposed neural network. The channel's real and imaginary parts are extracted separately, and then these two parts are connected into a tensor as an input to the network. Thus, the input to the neural network is T sequences of length $2L$.

The proposed network uses past and current information to estimate the current CSI. Thus, for channel estimation, there is an input for each time step of the GRU network. The input of the i-th GRU unit is denoted as:

$$x_i = \begin{cases} h_{GRU_{i-1}}(k) & \text{if } k \in K_d \\ h_{i-1}(k) & \text{if } k \in K_p, \end{cases} \tag{15}$$

where $h_{GRU_{i-1}}$ and h_{i-1} represent the CSI predicted by GRU and the CSI predicted by LS at the previous time step, respectively. K_d and K_p represent the data subcarrier and the pilot subcarrier, respectively. After that, x_i is handled by GRU:

$$h_{GRU_i} = GRU(x_i, \Theta), \tag{16}$$

where Θ represents all the parameters in the GRU.

In vehicular communication models, due to the fluctuating nature of CSI over time, the traditional GRU assigns the same weight to each feature in the model, which may lead to an uneven distribution of weights to features that have a greater impact at different stages, which may degrade the model performance. Therefore, by combining the attention mechanism with the GRU network, the probabilistic allocation properties of the attention mechanism can be utilized to assign higher weights to valid information and reduce the impact of redundant information.

As can be seen from the figure, the output of the GRU hidden layer is used as the input of the attention layer, which is calculated as follows:

$$E_t = \tanh(W_t h_{GRU_i} + b_t), \tag{17}$$

where E_t denotes the value of the probability distribution of attention determined by the hidden layer state vector h_{GRU_i} at moment t; W_t, b_t denote weights and bias, respectively. Then the attention weight value S_i of E_t can be expressed as:

$$S_i = \frac{e^{E_t}}{\sum_{j=0}^{i} e^{E_t}}. \tag{18}$$

Subsequently, the obtained S_i is multiplied with its corresponding input dimension h_{GRU_i} to obtain the output value of the attention mechanism:

$$r_i = \sum_{j=0}^{i} S_i h_{GRU_i}. \tag{19}$$

The final output is then reshaped into two $T \times L$ matrices as the real and imaginary parts of the final estimate. This step uses a fully connected layer to convert all hidden states into channel response estimates:

$$\hat{H} = W r_i + b, \tag{20}$$

where W, r_i, and b denote the weight matrix, hidden state after redistribution of weights by the attention mechanism, and bias vector, respectively. $\hat{H}$ is the final result of the channel estimation derived from the model.

B. TRAINING

Since the proposed network consists only of GRU units, the overall objective of the task is directly optimized without sub-module or stage training during the training process. Therefore, the final training results of the network are susceptible to the combination of hyperparameters. To alleviate this problem, this paper uses SSA to optimize the parameter settings of LSTM and GRU during offline training, which outperforms existing algorithms in terms of search accuracy, convergence speed, stability, and avoidance

of local optimization. In particular, it exhibits superior global optimization capabilities in complex solution environments [29], [30].

The SSA algorithm takes inspiration from the process of sparrow predation. Individuals called finders are responsible for finding food, the ultimate optimization target, and directing followers. Vigilantes are responsible for scouting for predators and alerting the population to avoid them. At each iteration, a fitness function is used to calculate each individual's fitness, where a high fitness means that it is closer to the optimal or better solution. The responsibilities of each individual also change depending on the fitness value. When the number of iterations is maximized, the individual with the highest fitness is regarded as the optimal solution [19]. The sparrow population matrix can be written as:

$$X = \begin{pmatrix} x_1^1 & x_1^2 & \dots & x_1^d \\ x_2^1 & x_2^2 & \dots & x_2^d \\ \vdots & \vdots & \ddots & \vdots \\ x_n^1 & x_n^2 & \dots & x_n^d \end{pmatrix}, \tag{21}$$

where x represents the individual sparrows, d refers to the number of hyperparameters to be optimized in the neural network, and n means the sparrows' number. The population fitness matrix is expressed as follows:

$$F_x = \begin{pmatrix} f([x_1^1 & x_1^2 & \dots & x_1^d]) \\ f([x_2^1 & x_2^2 & \dots & x_2^d]) \\ & \vdots & & \\ f([x_n^1 & x_n^2 & \dots & x_n^d]) \end{pmatrix}, \tag{22}$$

where $f(\cdot)$ denotes the fitness function of the individual sparrow. During the search process, highly adapted individuals become finders. They can prioritize searching a larger range of targets and approaching them, thus further guiding the whole group closer to the target. In each iteration, the finders are updated according to the following equation:

$$x_{i,d}^{t+1} = \begin{cases} x_{i,d}^t \cdot (1+Q) & \text{if } R < VT \\ x_{i,d}^t + Q & \text{if } R \geq VT, \end{cases} \tag{23}$$

where $x_{i,d}^{t+1}$ refer to the position of the i-th individual in the d-th dimension of the population in the $t+1$-th generation; Q is a standard normally distributed random number; R refer to a uniform random number in [0, 1], and VT refer to the vigilance threshold, which value in [0.5, 1.0]. $R \geq VT$ means the vigilant has detected a predator, and all individuals must be reset to a safe position. We can randomly generate the location of the vigilantes by using the following formula:

$$x_{i,d}^{t+1} = \begin{cases} x_{i,d}^t + \beta \cdot (x_{i,d}^t - xb_{i,d}^t) & \text{if } f_i \neq f_g \\ x_{i,d}^t + \beta \cdot (xw_{i,d}^t - xb_{i,d}^t) & \text{if } f_i = f_g, \end{cases} \tag{24}$$

where β is a random number that conforms to a standard normal distribution, xw is the current worst sparrow position, and xb is the current best sparrow position. f_i and f_g represent the present individual and global optimal fitness, respectively. That is, if the individual is currently in the best position, it will escape to a random position between the best and worst positions. Otherwise, it will flee to a random position between the current and best positions. At $R < VT$, when no predator is detected, the follower will gradually move closer to the finder and potentially become a new finder via the following formula:

$$x_{i,d}^{t+1} = xb_{i,d}^t + \frac{1}{D}\sum_{d=1}^{D}(rand\{-1, 1\} \cdot (|xb_{i,d}^t - x_{i,d}^t|)), \tag{25}$$

where xb is the best position of the individual in the population, D is the number of columns of the matrix A in the original equation. The matrix A is a $1 \times D$ matrix where each element is a random -1 or 1. Upon reaching the maximum iteration limit, the individual with the maximum global fitness among all is considered the optimal group of GRU hyperparameters. Table 3 shows the final training parameters.

TABLE 3. Network training parameters.

Paramenter	Values
Training sets	16000
Testing sets	4000
LSTM & GRU units	128
Epochs	150
Batch size	128
Loss function & Fitness function	MSE
Optimizer	Adam
Learning rate	0.01
Population size	10
Maximum Iterations	20
Vigilance threshold	0.8
Training SNR	40 dB

IV. SIMULATION

This paper compares CNN [32], LSTM [23], SSA-LSTM, GRU [33], SSA-GRU, and the proposed SSA-GRU-Att estimator simulation results, where the SSA-LSTM and SSA-GRU estimators are improved according to Ref. [23] and Ref. [33]. Two main types of V2V channel models are generally used: geometry-based channel models and tapped delay line models (TDL). Although the geometric model describes the V2V channel characteristics more accurately, the complexity is excessive. In contrast, the TDL model can roughly describe the V2V channel characteristics with lower complexity [31], so the TDL model is introduced. Two classical scenarios are selected for the channel model: 1) Vehicle-to-Vehicle Same Direction With Wall (VTV-SDWW), which indicates that the channel between vehicles traveling on a highway is separated by a wall and is suitable for highly dynamic vehicular environments. The Doppler shifts are $f_d = 550$ Hz and $f_d = 1100$ Hz, representing speeds of 100 km/h and 200 km/h, respectively. 2) Vehicle-to-Vehicle Urben Canyon (VTV-UC) describes a roadway with high-rise buildings or canyons on both sides. The vehicle speed is 48 km/h, equivalent to $f_d = 250$ Hz. A frame size of 20 OFDM symbols is used for simulation. The main parameters of the simulation environment are summarized in Table 4.

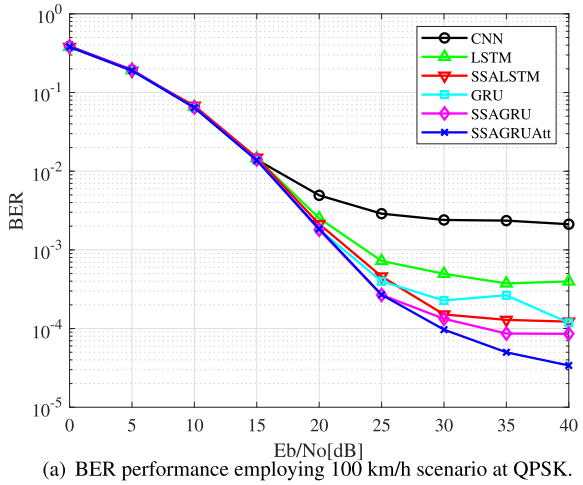

(a) BER performance employing 100 km/h scenario at QPSK.

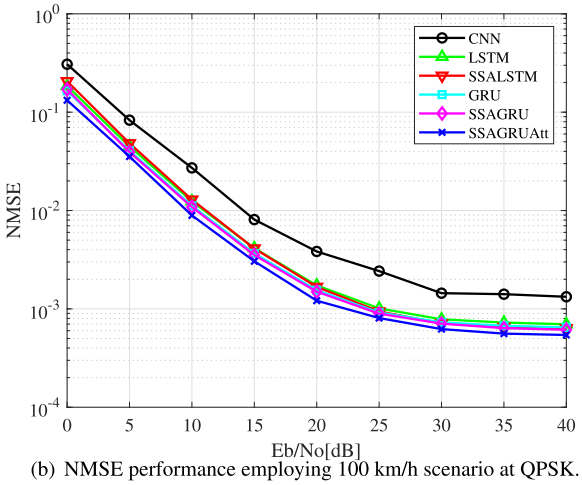

(b) NMSE performance employing 100 km/h scenario at QPSK.

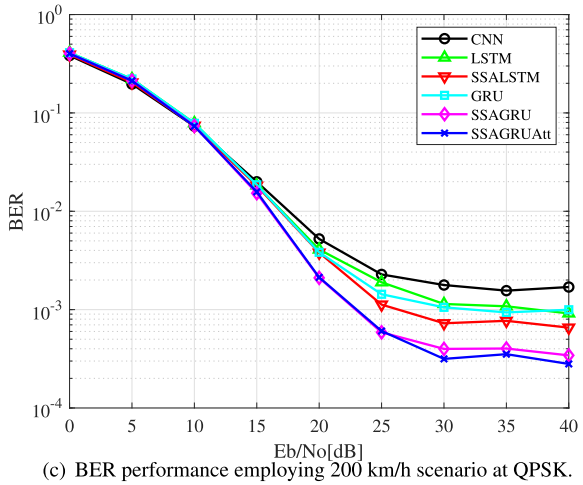

(c) BER performance employing 200 km/h scenario at QPSK.

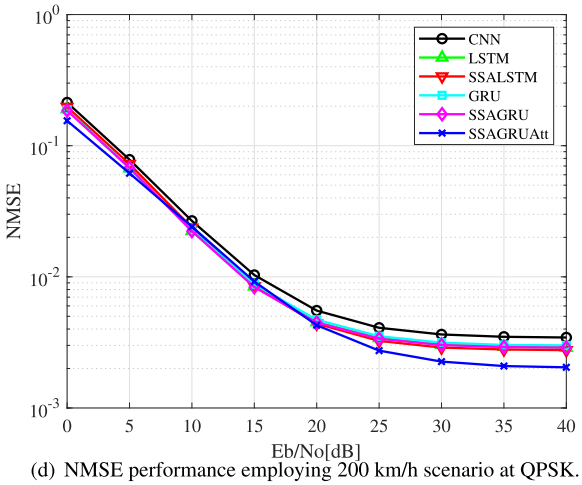

(d) NMSE performance employing 200 km/h scenario at QPSK.

FIGURE 4. VTV-SDWW vehicular channel model simulation results.

TABLE 4. Simulation parameters.

Paramenter	Values
Carrier frequency	5.9 GHz
Bandwidth	10 MHz
FFT size & Total subcarriers	64
Number of data subcarriers	48
Number of pilot subcarriers	4
Modulation	QPSK, 16QAM, 64QAM
OFDM symbol duration	8 μs
FFT/IFFT period	6.4 μs
Guard interval duration	1.6 μs
Number of OFDM symbols per frame	20
Channel model	VTV-SDWW, VTV-UC
Channel taps	12
Subcarrier spacing	156.25 kHz
Vehicle speed	48 km/h, 100 km/h, 200 km/h
Maximum Doppler shift	250 Hz, 550 Hz, 1100 Hz

A. BER AND NMSE PERFORMANCE

Fig. 4 illustrates each model's BER and NMSE performance. We can find that LSTM and GRU-based estimators outperform CNN-based estimators. This is because the NLP approach is more advantageous when dealing with sequential problems. The CNN estimator, on the other hand, is affected by the error substrate and performs poorly in the high SNR region. It can be found that in the lower SNR region, the BER performance of all methods is similar. This is due to the fact that under low SNR conditions, the effect of noise on the system performance is dominant and the noise component in the received signal is significantly enhanced, resulting in difficulties for the receiver to accurately demodulate the transmitted signal.

Meanwhile, it can be found that SSA-LSTM is better than LSTM in the high SNR region. In Fig. 4(a), the LSTM and GRU estimator optimized by the SSA algorithm can outperform the LSTM and GRU estimator by 9 dB and 3 dB of gain in a high-speed environment in terms of SNR at BER $= 3 \times 10^{-3}$. This proves the effectiveness of SSA for neural network optimization. Moreover, the SSA-GRU estimator outperforms the SSA-LSTM in the entire SNR region, which can be explained by the GRU's higher training efficiency, resulting in a stronger ability to

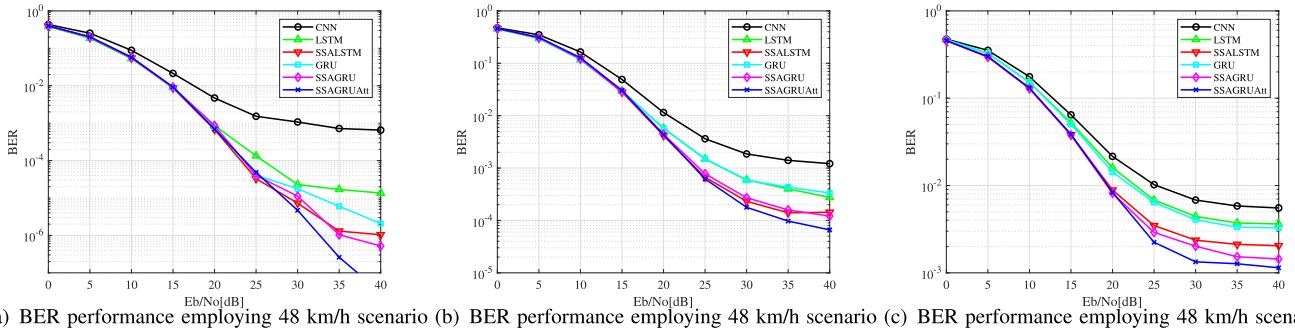

(a) BER performance employing 48 km/h scenario at QPSK. (b) BER performance employing 48 km/h scenario at 16QAM. (c) BER performance employing 48 km/h scenario at 64QAM.

FIGURE 5. VTV-UC vehicular channel model simulation results.

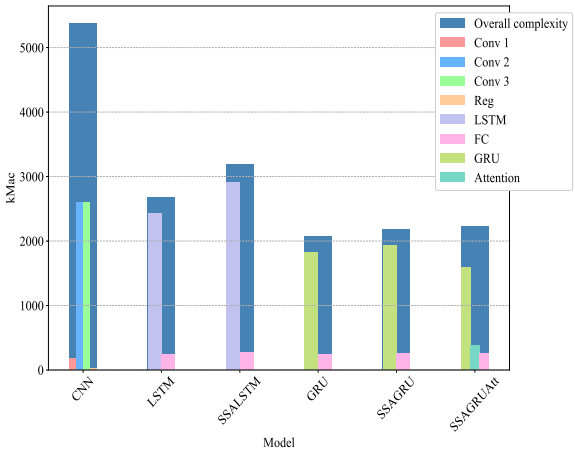

FIGURE 6. MACs used by each estimator for channel estimation.

learn channel temporal correlations. In addition, The SSA-GRU-Att estimator outperforms the SSA-GRU estimator by 3 dB of gain in terms of SNR at BER $= 10^{-4}$. This demonstrates the ability of the model to better focus on relevant channel state information and improve the quality of the feature representation, which is particularly important for dealing with rapidly changing channel conditions in high-mobility scenarios.

Fig. 4(c) illustrates the BER performance of each model at higher speeds. Compared to the relative speed of 100km/h, all the estimators have some degree of performance degradation, which is due to the fact that with the increase of the Doppler frequency shift, the channel varies more drastically in time and at the same time the frequency expansion leads to more serious inter-signal interference (ISI). In contrast, the proposed SSA-GRU and SSA-GRU-Att estimators are able to outperform the SSA-LSTM estimator by 4db gain at BER $= 10^{-3}$. This is due to the fact that LSTM employs long-term memory, so the estimation results for the current channel are affected by channels estimated earlier. As the speed increases, the channels at consecutive OFDM symbols may become uncorrelated, which can impair the performance of the LSTM estimator even more. However, the SSA-GRU-Att estimator still has better BER performance than other deep learning-based schemes, which indicates that the SSA-GRU-Att estimator can capture the temporal correlation of the channel better and thus performs better in highly dynamic environments.

Fig. 4(b) and Fig. 4(d) illustrate the NMSE performance of each estimator. From the simulation results, the LSTM-based and GRU-based estimators perform similarly, but all of them outperform the CNN-based estimator, which demonstrates that NLP-based methods have a better understanding of channel conditions, allowing for more efficient signal processing. Whereas estimators other than the CNN-based estimator perform close, this is due to the fact that the loss function is based on NMSE and the model prefers to minimize the error overall. Despite the NMSE proximity, the difference in BER suggests that the models differ in their ability to capture the complex characteristics of the channel and dynamically adjust their estimation strategies. As for the very high mobility scenario, the performance of each model tends to be similar, but the SSA-GRU-Att estimator exhibits lower NMSE values, which indicates its better error control ability in dealing with highly dynamic environments. Meanwhile, the SSA-GRU-Att estimator also exhibits lower NMSE values at lower signal-to-noise ratios, indicating that it performs better in noisy situations.

Fig. 5 shows the BER performance of each estimator for different modulation methods in the VTV-UC channel. It can be found that the SSA-LSTM, SSA-GRU, and SSA-GRU-Att estimators achieve similar performance in low-mobility scenarios due to the negligible effect of Doppler interference in low-mobility scenarios. However, in the high SNR region, SSA-GRU-Att has a higher potential. For 16QAM and 64QAM, the proposed estimator outperform the SSA-LSTM estimator about 5 db gain at BER $= 10^{-4}$ and BER $= 2 \times 10^{-3}$, respectively. This demonstrates that the attention mechanism can enhance the model's ability to capture channel state information.

B. COMPUTATIONAL COMPLEXITY ANALYSIS

This section presents a detailed computational complexity analysis of the channel estimation scheme. Since a large number of computations in all estimators are multiplicative and additive operations, multiply-accumulate operation (MAC) is

TABLE 5. MACs and execution time used by each estimator for channel estimation.

Channel estimator	MACs	Execution time
CNN	5.38 M	3.7951 ms
LSTM	2.67 M	1.8561 ms
SSA-LSTM	3.19 M	2.2492 ms
GRU	2.06 M	1.4428 ms
SSA-GRU	2.18 M	1.5448 ms
SSA-GRU-Att	2.23 M	1.5509 ms

used to evaluate the computational complexity of each model. In addition to this, the execution times of the individual estimators are compared.

Since LSTM-based and GRU-based estimators estimate each symbol individually, CNN-based estimators process the whole frame simultaneously. The simulation results are based on the estimation for the entire OFDM frame. Figure 6 and Table 5 show the overall complexity of each estimator as well as the complexity of each layer, and the execution time of each estimator, respectively. It can be found that the CNN-based channel estimator requires a large number of MACs because the convolutional layers involve a large number of convolutional operations. In addition, it is difficult to find a good balance of complexity and performance for LSTM-based channel estimators. This is because LSTMs have additional gating mechanisms and separate memory cells, which, while making LSTMs more powerful in capturing long-time dependencies, also increases the computational complexity. In contrast, the proposed SSA-GRU-Att channel estimator ensures better reliability with relatively low computational complexity.

V. CONCLUSION

In this paper, we propose an optimization method based on GRU and SSA for channel estimation in vehicular communication and incorporate an attention mechanism to filter redundant information and improve accuracy. Experimental results validate the effectiveness of this approach, showing improved channel estimation accuracy and reduced complexity. Limitations include the lack of real V2V testing and the performance in very high-speed scenarios that still need further investigation. Although the computational complexity has been reduced, further consideration needs to be given to deployment on resource-limited vehicle terminals. Future work will aim to validate the model in real V2V scenarios and enhance its adaptability to complex channels with strong multipath effects or severe interference.

REFERENCES

[1] H. P. D. Nguyen and R. Zoltán, "The current security challenges of vehicle communication in the future transportation system," in *Proc. IEEE 16th Int. Symp. Intell. Syst. Informat. (SISY)*, Sep. 2018, pp. 161–166.

[2] A. Maimaris and G. Papageorgiou, "A review of intelligent transportation systems from a communications technology perspective," in *Proc. IEEE 19th Int. Conf. Intell. Transp. Syst. (ITSC)*, Nov. 2016, pp. 54–59.

[3] A. Daniel, A. Paul, A. Ahmad, and S. Rho, "Cooperative intelligence of vehicles for intelligent transportation systems (ITS)," *Wireless Pers. Commun.*, vol. 87, no. 2, pp. 461–484, Mar. 2016.

[4] M. N. O. Sadiku, N. Gupta, and K. K. Patel, "An overview of intelligent transportation systems in the context of Internet of Vehicles," in *Internet of Vehicles and Its Applications in Autonomous Driving*. Berlin, Germany: Springer, 2021, pp. 3–11.

[5] Y. Liao, Y. Hua, X. Dai, H. Yao, and X. Yang, "ChanEstNet: A deep learning based channel estimation for high-speed scenarios," in *Proc. IEEE Int. Conf. Commun. (ICC)*, Shanghai, China, May 2019, pp. 1–6.

[6] A. A. Almohammedi, N. K. Noordin, A. Sali, F. Hashim, and M. Balfaqih, "An adaptive multi-channel assignment and coordination scheme for IEEE 802.11P/1609.4 in vehicular ad-hoc networks," *IEEE Access*, vol. 6, pp. 2781–2802, 2018.

[7] S. Johari and M. B. Krishna, "Time-slot reservation and channel switching using Markovian model for multichannel TDMA MAC in VANETs," *IEEE Access*, vol. 10, pp. 81250–81268, 2022.

[8] P. Alexander, D. Haley, and A. Grant, "Cooperative intelligent transport systems: 5.9-GHz field trials," *Proc. IEEE*, vol. 99, no. 7, pp. 1213–1235, Jul. 2011.

[9] K. K. Nagalapur, F. Brännström, E. G. Ström, F. Undi, and K. Mahler, "An 802.11p cross-layered pilot scheme for time- and frequency-varying channels and its hardware implementation," *IEEE Trans. Veh. Technol.*, vol. 65, no. 6, pp. 3917–3928, Jun. 2016.

[10] S. In Kim, H. S. Oh, and H. K. Choi, "Mid-amble aided OFDM performance analysis in high mobility vehicular channel," in *Proc. IEEE Intell. Vehicles Symp.*, Eindhoven, The Netherlands, Jun. 2008, pp. 751–754.

[11] M. A. R. Jeich and K. U. O. Chi-Cheng, "Performance improvement of the DSRC system using a novel S and π-decision demapper," *Wireless Sensor Netw.*, vol. 1, no. 4, p. 268, 2009.

[12] A. Bourdoux, H. Cappelle, and A. Dejonghe, "Channel tracking for fast time-varying channels in IEEE802.11p systems," in *Proc. IEEE Global Telecommun. Conf. GLOBECOM*, Dec. 2011, pp. 1–6.

[13] Y. Du, D. Rajan, and J. Camp, "Implementation and evaluation of channel estimation and phase tracking for vehicular networks," in *Proc. 9th Int. Wireless Commun. Mobile Comput. Conf. (IWCMC)*, Jul. 2013, pp. 1263–1268.

[14] J. A. Fernandez, K. Borries, L. Cheng, B. V. K. V. Kumar, D. D. Stancil, and F. Bai, "Performance of the 802.11p physical layer in vehicle-to-vehicle environments," *IEEE Trans. Veh. Technol.*, vol. 61, no. 1, pp. 3–14, Jan. 2012.

[15] Z. Zhao, X. Cheng, M. Wen, B. Jiao, and C.-X. Wang, "Channel estimation schemes for IEEE 802.11p standard," *IEEE Intell. Transp. Syst. Mag.*, vol. 5, no. 4, pp. 38–49, Winter. 2013.

[16] Y.-K. Kim, J.-M. Oh, Y.-H. Shin, and C. Mun, "Time and frequency domain channel estimation scheme for IEEE 802.11p," in *Proc. 17th Int. IEEE Conf. Intell. Transp. Syst. (ITSC)*, Qingdao, China, Oct. 2014, pp. 1085–1090.

[17] H. Ye, G. Y. Li, and B.-H. Juang, "Power of deep learning for channel estimation and signal detection in OFDM systems," *IEEE Wireless Commun. Lett.*, vol. 7, no. 1, pp. 114–117, Feb. 2018.

[18] C. Qing, L. Dong, L. Wang, J. Wang, and C. Huang, "Joint model and data-driven receiver design for data-dependent superimposed training scheme with imperfect hardware," *IEEE Trans. Wireless Commun.*, vol. 21, no. 6, pp. 3779–3791, Jun. 2022.

[19] H. He, J.-H. Wang, S. Kojima, K. Maruta, and C.-J. Ahn, "Regression CNN based fast fading channel tracking using decision feedback channel estimation," *J. Signal Process.*, vol. 27, no. 3, pp. 49–57, 2023.

[20] W. Yin, K. Kann, M. Yu, and H. Schütze, "Comparative study of CNN and RNN for natural language processing," 2017, *arXiv:1702.01923*.

[21] C. Zhou, C. Sun, Z. Liu, and F. C. M. Lau, "A C-LSTM neural network for text classification," 2015, *arXiv:1511.08630*.

[22] D. W. Otter, J. R. Medina, and J. K. Kalita, "A survey of the usages of deep learning for natural language processing," *IEEE Trans. Neural Netw. Learn. Syst.*, vol. 32, no. 2, pp. 604–624, Feb. 2021.

[23] A. K. Gizzini, M. Chafii, S. Ehsanfar, and R. M. Shubair, "Temporal averaging LSTM-based channel estimation scheme for IEEE 802.11p standard," in *Proc. IEEE Global Commun. Conf. (GLOBECOM)*, Dec. 2021, pp. 1–7.

[24] J. Pan, H. Shan, R. Li, Y. Wu, W. Wu, and T. Q. S. Quek, "Channel estimation based on deep learning in vehicle-to-everything environments," *IEEE Commun. Lett.*, vol. 25, no. 6, pp. 1891–1895, Jun. 2021.

[25] T. Zhou, H. Zhang, B. Ai, C. Xue, and L. Liu, "Deep-learning-based spatial–temporal channel prediction for smart high-speed railway communication networks," *IEEE Trans. Wireless Commun.*, vol. 21, no. 7, pp. 5333–5345, Jul. 2022.

[26] Y. Yanlei, "Cloud edge linkage optimization of process manufacturing process parameters integrating GRU-attention and whale algorithm," *Comput. Integr. Manuf. Syst.*, vol. 29, no. 9, p. 2991, 2023.
[27] N. Unnisa and M. Tatineni, "Adaptive deep learning strategy with red deer algorithm for sparse channel estimation and hybrid precoding in millimeter wave massive MIMO-OFDM systems," *Wireless Pers. Commun.*, vol. 122, no. 4, pp. 3019–3051, Feb. 2022.
[28] J. Chung, C. Gulcehre, K. Cho, and Y. Bengio, "Empirical evaluation of gated recurrent neural networks on sequence modeling," 2014, *arXiv:1412.3555*.
[29] J. Xue and B. Shen, "A novel swarm intelligence optimization approach: Sparrow search algorithm," *Syst. Sci. Control Eng.*, vol. 8, no. 1, pp. 22–34, Jan. 2020.
[30] J. Madiniyeti, Y. Chao, T. Li, H. Qi, and F. Wang, "Concrete dam deformation prediction model research based on SSA–LSTM," *Appl. Sci.*, vol. 13, no. 13, p. 7375, Jun. 2023.
[31] D. W. Matolak, I. Sen, and W. Xiong, "Channel modeling for V2V communications," in *Proc. 3rd Annu. Int. Conf. Mobile Ubiquitous Syst. Workshops*, San Jose, CA, USA, Jul. 2006, pp. 1–7.
[32] A. K. Gizzini, M. Chafii, A. Nimr, and G. Fettweis, "Joint TRFI and deep learning for vehicular channel estimation," in *Proc. IEEE Globecom Workshops (GC Wkshps*, Dec. 2020, pp. 1–6.
[33] J. Hou, H. Liu, Y. Zhang, W. Wang, and J. Wang, "GRU-based deep learning channel estimation scheme for the IEEE 802.11p standard," *IEEE Wireless Commun. Lett.*, vol. 12, no. 5, pp. 764–768, May 2023.

JUN-HAN WANG received the B.E. degree in electrical and electronics engineering from Dalian Maritime University, Dalian, China, in 2018, and the M.E. degree in informatics and data science from Hiroshima University, Hiroshima, Japan, in 2020. He is currently pursuing the Ph.D. degree with Chiba University. His research interests include machine learning and the development of vehicle-to-everything algorithms. He received the ICEIC Best Paper Award, in 2024.

HE HE received the B.E. degree in electrical and electronics engineering from Dalian Maritime University, Dalian, China, in 2018, and the M.E. and Ph.D. degrees in electrical and electronics engineering from Chiba University, Chiba, Japan, in 2020 and 2023, respectively. He is currently a Researcher with Honda. His research interests include machine learning and the development of next-generation communication algorithms.

KOSUKE TAMURA (Graduate Student Member, IEEE) received the B.E. degree from Chiba University, Japan, in 2023, where he is currently pursuing the M.E. degree in electrical and electronics engineering. His research interests include OFDM, SEFDM, MIMO, and machine learning-based wireless communication systems. He received the Best Paper Award at the International Conference on Electronics, Information, and Communication (ICEIC), in 2024, and the IEEE VTS Tokyo/Japan Chapter 2024 Young Researcher's Encouragement Award.

SHUN KOJIMA (Member, IEEE) received the B.E., M.E., and Ph.D. degrees in electrical and electronics engineering from Chiba University, Japan, in 2017, 2018, and 2021, respectively. From 2021 to 2022, he was an Assistant Professor with the Department of Fundamental Engineering, Utsunomiya University, Tochigi, Japan. He is currently a Project Research Associate with the Institute of Industrial Science, The University of Tokyo, Tokyo, Japan. His research interests include adaptive modulation and coding, visible light communications, physical layer security, and machine learning. He received the Best Paper Award at the 26th International Conference on Software, Telecommunications and Computer Networks, in 2018, the Best Poster Award at the 3rd Communication Quality Student Workshop, in 2019, the IEEE VTS Tokyo/Japan Chapter 2020 Young Researcher's Encouragement Award, the RISP Best Paper Award, in 2021, the Institute of Electronics, Information and Communication Engineers (IEICE) Radio Communication Systems Active Researcher Award, in 2021, the IEICE Young Researchers Award, in 2023, and the Takayanagi Research Encouragement Award, in 2023.

JAESANG CHA received the Ph.D. degree from the Department of Electronic Engineering, Tohoku University, Japan, in 2000. He was with ETRI, from 2000 to 2002, with Seokyeong University, from 2002 to 2005, and with SNUST, from 2005 to 2020. Since 2023, he has been a Professor in Chiba, Japan. His research interests include wireless communication, the IoT, and IT convergence technology.

CHANG-JUN AHN (Senior Member, IEEE) received the Ph.D. degree from the Department of Information and Computer Science, Keio University, Japan, in 2003. From 2001 to 2003, he was a Research Associate with the Department of Information and Computer Science, Keio University. From 2003 to 2006, he was with the Communication Research Laboratory, Independent Administrative Institution (now the National Institute of Information and Communications Technology). In 2006, he was on assignment with the ATR Wave Engineering Laboratories. In 2007, he was with the Faculty of Information Sciences, Hiroshima City University, as a Lecturer. From 2019 to 2021, he was with the Electrical and Computer Engineering, Duke University, as a Visiting Professor. He is currently with the Graduate School of Engineering, Chiba University, as a Professor. His research interests include OFDM, MIMO, digital communication, channel coding, and signal processing for telecommunications. From 2005 to 2006, he was an Expert Committee Member for Emergence Communication Committee, Shikoku Bureau of Telecommunications, Ministry of Internal Affairs and Communications (MIC), Japan. From 2010 to 2016, he was a Technical Committee Member of IEICE. From 2021 to 2023, he was an Editor of *IEICE Transactions*. He is a Senior Member of IEICE. He received the ICF Research Award for Young Engineer, in 2002, the Funai Information Science Award for Young Scientist, in 2003, the Distinguished Service Award from Hiroshima City, in 2010, IEEE SoftCOM 2018 Best Paper Award, IEEE APCC 2019 Best Paper Award, IEICE ICETC 2020 Best Paper Award, Journal of Signal Processing Best Paper Award, in 2021, IEEE ICCE-Asia 2022 Best Paper Award, IEEE ISAAC 2023 Best Paper Award, and IEEE ICEIC2024 Best Paper Award.